Turkish Journal of Earth Sciences (Turkish J. Earth Sci.), Vol. 19, 2010, pp. 351–366. Copyright ©TÜBİTAK
doi:10.3906/yer-0812-8 First published online 25 August 2010

Tsunami Hazard Assessment on the Southern Coast of Spain

MAURICIO GONZALEZ[1], RAÚL MEDINA[1], MAITANE OLABARRIETA[1] & LUIS OTERO[2]

[1] Ocean & Coastal Research Group, Instituto de Hidráulica Ambiental 'IH Cantabria' Universidad de Cantabria, E.T.S.I. Caminos Canales y Puertos. Avda. de los Castros s/n 39005, Santander, Spain
(E-mail: gonzalere@unican.es)

[2] Dirección General Marítima. Ministerio de Defensa Nacional, Armada Nacional. Av. El Dorado CAN, Bogota, Colombia

Received 22 January 2009; revised typescript receipt 24 August 2009; accepted 04 August 2010

Abstract: In this study an indirect statistical method has been proposed to estimate the tsunami hazard assessment along the Alborán Sea Coast (Southeastern Spanish Coast). This method can be summarized as: (1) analysis of the global neotectonic setting, including geodynamic processes as well as seismicity of the region; (2) tsunami source model; (3) generation of a numerical data base of tsunami events using a numerical model; (4) probabilistic model based on Monte-Carlo simulations in order to generate a synthetic tsunami catalogue; and (5) a multidimensional interpolation method applied to combine the numerical data base with the synthetic catalogue to produce inundation maps. The purpose of this study is to establish tsunami-wave elevation at the shoreline versus the return period curves for different locations along the Alborán Sea coast. Furthermore, an inundation map of the city of Roquetas del Mar (Almeria) has been obtained. It is concluded that the tsunamis generated in the Alborán basin have a medium to low hazard, with the most important elevations in the Málaga, Adra and Melilla areas.

Key Words: tsunami, Alborán Sea, Monte-Carlo, tsunami hazard assessment, propagation modelling

İspanya Güney Sahilleri İçin Tsunami Tehlikesinin Değerlendirilmesi

Özet: Bu çalışmada Alborán Denizi sahillerindeki (Güneydoğu İspanya sahilleri) tsunami tehlikesinin değerlendirilmesi için bir dolaylı istatiksel yöntem önerilmektedir. Yöntem şöyle özetlenebilir: (1) jeodinamik prosesler ile çalışma bölgesinin sismitesini de içeren küresel neotektonik rejimin bir değerlendirilmesi; (2) tsunami kaynak modeli; (3) sayısal model kullanarak tsunami olayları için sayısal veri tabanının oluşturulması; (4) sintetik tsunami kataloğunun oluşturulması için Monte-Carlo similasyonlarına göre olasılıklı model geliştirilmesi; ve (5) sayılsal veri tabanı ile sintetik kataloğun birleştirilmesiyle su baskını haritalarının üretilmesi için çok boyutlu iç değerleme/enterpolasyon yönteminin uygulanması. Bu çalışmanın amacı sahil şeridindeki tsunami-dalga yüksekliği ile Alborán Denizi kıyısı boyunca değişik yerler için geri dönüş peryot eğrilerini karşılaştırmalı olarak tesis edilmesidir. Bundan başka, Roquetas del Mar (Almeria) şehri için su baskını haritasıda oluşturuldu. Sonuç olarak Alborán havzasında oluşacak tsunamilerin orta-az tehlikeli olacakları, en yüksek su seviyesinin Málaga, Adra and Melilla bölgelerinde oluşacağı önerilmektedir.

Anahtar Sözcükler: tsunami, Alborán Denizi, Monte-Carlo, tsunami tehlike değerlendirmesi, yayılma modeli

Introduction

The Alborán seacoast is located by the southwestern Mediterranean Sea and occasionally this area is affected by tsunamis (see Figure 1 where some historical tsunamigenic epicenters are shown).

During the last few decades, the southeastern coast of Spain (Almería, Málaga and Marbella) has suffered an enormous transformation due to the tourism boom and the demand for coastal use. For this reason, a great number of infrastructures have

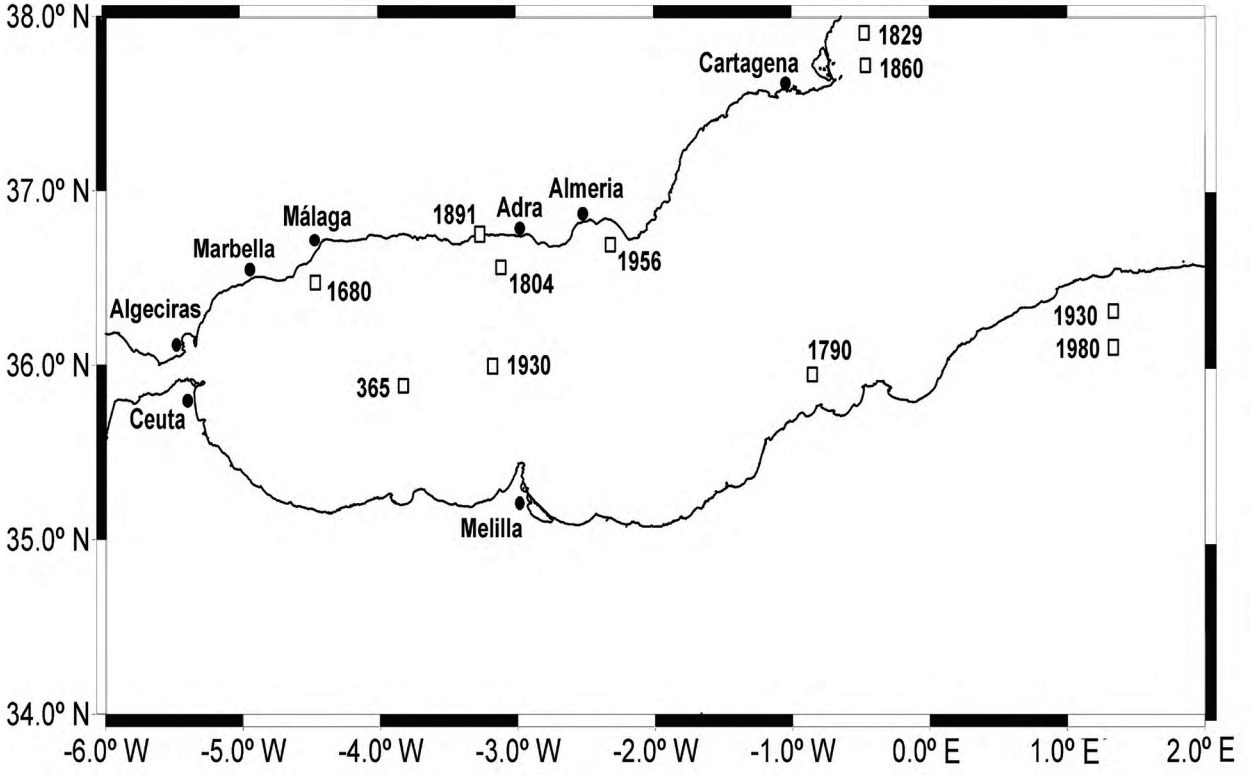

Figure 1. Historical tsunamigenic events.

been built (marinas, beaches, highways, boardwalks, hotels, etc.), which could be affected by tsunamis. The objective of this study is to establish the tsunami wave elevation hazard along the Alborán Sea. Since the frequency of occurrence, location, and magnitude of tsunamigenic earthquakes are random, the tsunami hazard analyses must be based on probabilistic considerations.

Tsunami hazard can be analysed from the deterministic and probabilistic points of view. The first case consists of taking the worst credible tsunami case, which is usually derived from the historical tsunami data in the study zone. In the second case, the probabilistic point of view, a selected series of tsunami events are combined using empirical or computational methods. The selection of each approach greatly depends on the objectives of the hazard analysis which can be summarized as follows: (1) to condense the complexity and the variability of tsunamis into a manageable set of parameters, and (2) to provide a synopsis of the tsunami hazard along entire coastlines in order to help identify vulnerable locations along the coast and specific tsunami source regions to which these vulnerable locations on the coastline are sensitive (Geist & Parsons 2006).

The probabilistic empirical analysis is carried out in a particular location where historical records of tsunami run-up and amplitude data are available. A priori knowledge of source type is not needed to calculate probabilities (Papadoupoulos 2003). However, probabilistic computational-based methods rely on the knowledge of source parameters, recurrence rates and their uncertainties. The advantage of computational methods compared to empirical ones, is that they can be applied in regions with scant historical records and can include parameter sensitivity estimates in the analysis. Because in most places around the world historical tsunami run-up records are scarce, computational-based Probabilistic Tsunami Hazard Analysis (PTHA) is usually applied.

The main difference between the different computational PTHA relies on the fact that some of them are used to analyse the tsunami hazard in a specific zone of the coastal region (Rikitake & Aida 1988; Ward 2001). However, other methods, like the Monte-Carlo based methods or logic-tree approaches (Annaka *et al.* 2007) are used to analyse the hazard in a whole coastal region.

Monte-Carlo techniques are useful for including multiple sources of uncertainty in hazard analysis (Savage 1992; Cramer *et al.* 1996; Ebel & Kafka 1999). This method allows uncertainties in the input parameters to be dealt with in a very powerful way; parameters can be entered as distribution functions with observed mean and standard deviations. A different value can be sampled from the distribution for each simulation. This approach is more attractive than the use of a logic-tree, where the choice of weights for each branch in the tree tends to be subjective (Musson 2000).

Given that the catalogue of tsunamis that have occurred along the Alborán Sea coast includes only a few events, since tsunamis are rather infrequent and in the past, scientific attention to these natural phenomena was scarce or even absent in the Alborán seacoast as in many other countries, in this paper we will apply a probabilistic methodology based on Monte-Carlo numerical simulations for the tsunami hazard assessment in the Alborán Sea.

Monte-Carlo simulation involves using a large statistical sample in calculating initial conditions for a numerical model. To determinate tsunami recurrence rates and probabilities, the method can be summarized as a combination of different procedures:

- Selection of the tsunamigenic sources and seismic parameters.
- A tsunami source model (seismological model).
- Event simulations with a hydrodynamic numerical model.
- Probabilistic Tsunami Hazard Analysis (PTHA).

Tsunamigenic Sources

Taking into account the global neotectonic setting, the geodynamic processes as well as the seismicity of the considered region, it is possible to determine potential tsunamigenic sources, whether or not they are historically active. It is likely that the major cause of catastrophic tsunamis is underwater shallow focus earthquakes of Richter magnitude 5.0 or greater (Iida 1963, 1970). However, not all such earthquakes produce tsunamis since the generation mechanism is usually associated with vertical dislocations of the sea floor in dip-slip normal or reverse faults.

Neotectonic Features

The Alborán Sea in the southwestern Mediterranean is a very active region in the wide area of continental collision generated by the northward movement of the African Plate relative to the European Plate (Dewey *et al.* 1989). The unusual tectonic situation of a small sea caught between two major plates is characterized by a complex sea floor topography, with several basins separated by structural heights and ridges (Maldonado *et al.* 1992a, b; Woodside *et al.* 1992). Furthermore, some authors (Udías *et al.* 1976, 1992; Mezcua & Rueda 1997; Meghraoui *et al.* 2004) have proposed different geodynamic models based on source mechanisms of earthquakes that permit the determining of the fault system in the Alborán Sea. The tectonic features are characterized by a fault system composed of short strike-slip faults and short dip-slip faults, as shown in Figure 2. This short fault system is due to the crustal shocks of the African and European plates, where a benioff or subduction zone is not evident.

Seismic Pattern

The spatial distribution of seismicity could be considered a manifestation of the lithospheric weakness zone where the stresses applied are released, that, joined with some seismic parameters, permit the determination of potential tsunamigenic sources. The Alborán Sea presents high seismic activity, with moderate earthquake magnitudes and shallow epicentres. The earthquakes are associated with the local fault system.

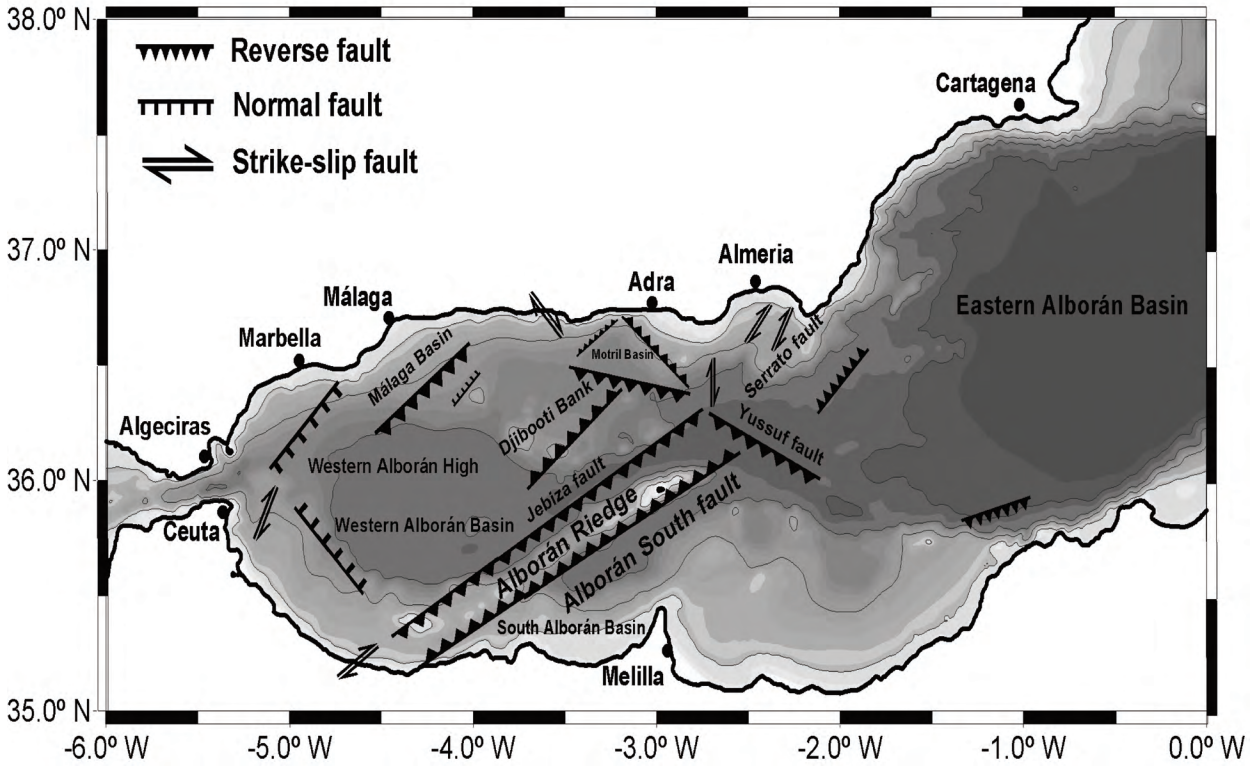

Figure 2. Schematic summary of principal neotectonic and geomorphologic elements in the Alborán Sea.

The data for the earthquakes were taken from: (1) the Spanish National Seismic Catalogue from the period 1916–2006: (2) the Spanish seismic hazard maps from the National Geographic Institute (NGI) from the period 1320–1920. In Figure 3, different Richter magnitudes of the earthquakes from the 1916–2006 period are shown for ($M_s \geq 5.0$).

Potential Faults

Five potential tsunamigenic sources have been selected for the Alborán Sea, taking into account: (1) the historical tsunami data (Figure 1); (2) the analysis of the dip-slip faults (normal and reverse); and (3) analysis of seismicity. This kind of analysis is used as an important tool to estimate the potential for tsunamigenic earthquakes (Alami & Tinti 1991). Only the seismic data with a magnitude greater than 5.0 on the Richter scale with focal depths between 50 km and 20 km are included in the analysis (Iida 1963, 1970).

Tsunamis of distant origin (Italian and Greek sources) are not considered a threat to the study area. Furthermore, although Atlantic Ocean sources (Azores-Gibraltar fault system) can generate great tsunamis, they do not cause any perceivable perturbations in the Alborán Sea. Historical events and numerical simulations confirm that the Strait of Gibraltar acts as an important tsunami filter.

Finally, the eastern Algerian sources have been studied by different authors in order to analyze tsunami hazard in the Balearic Islands (Wang & Liu 2005; Alasset *et al.* 2006; Álvarez-Gómez *et al.* 2010). However, these tsunami sources have not been included because their influence in the Alborán Sea area is not relevant, as numerical simulations have confirmed. As an example, the numerical simulation of the tsunami induced by the 2003 Boumerdes-Zemmouri Earthquake (Mw= 6.9, Algeria) is shown in Figure 4, where the maximum tsunami wave height is presented in different locations at 6 m water depth (see locations in Figure 5). The fault plane

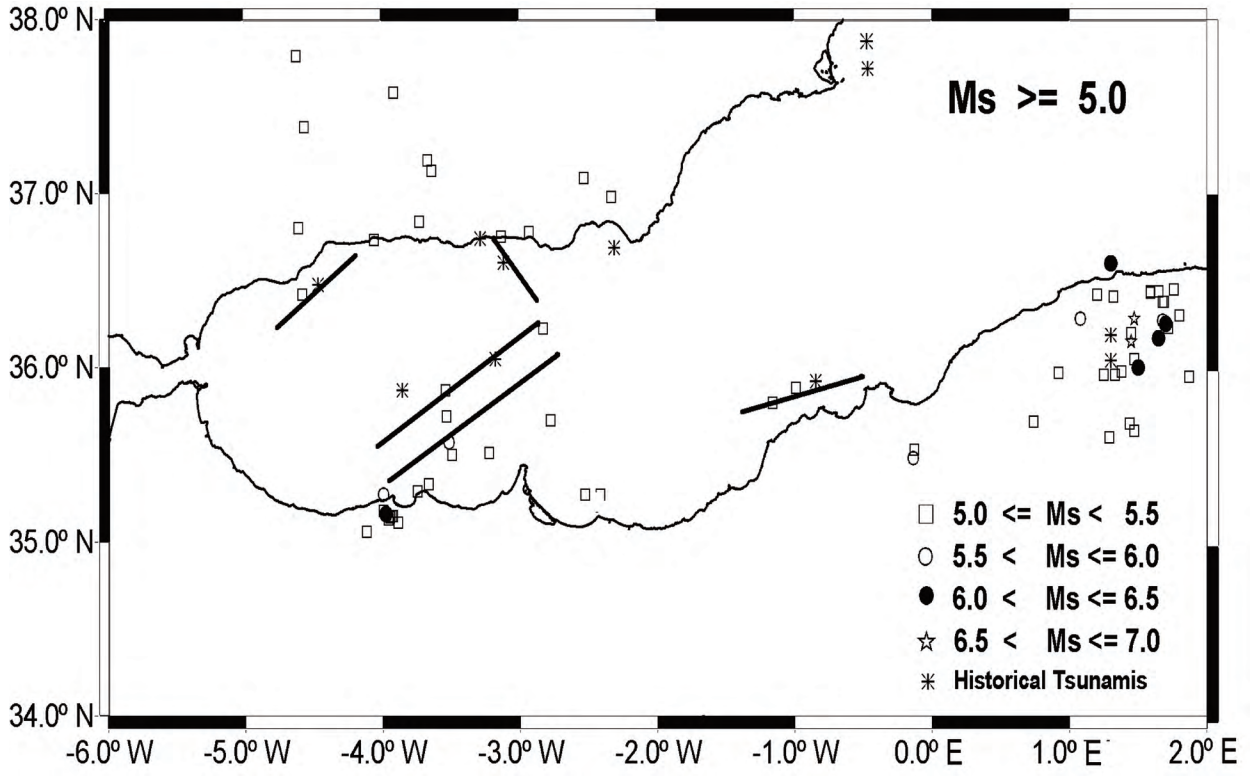

Figure 3. Relocated seismicity (M_s 5.0), for the period 1916–2002 and potential tsunamigenic sources.

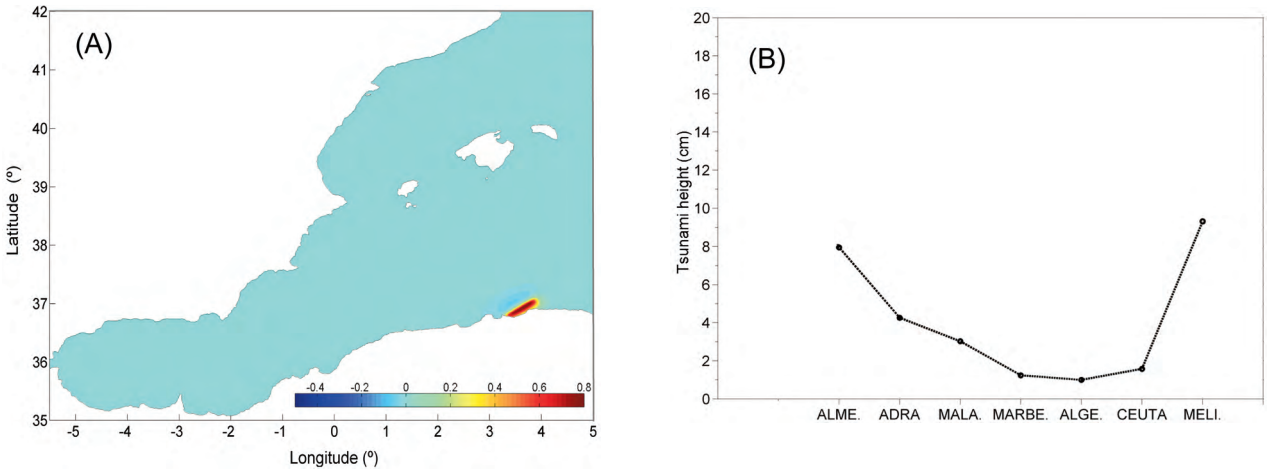

Figure 4. **(A)** Initial free surface deformation produced by the 2003 Boumerdes-Zemmouri earthquake (Mw= 6.9, Algeria), **(B)** Maximum Tsunami wave height in 6-m-water depth in Cartagena, Almería, Adra, Málaga, Marbella, Algeciras, Ceuta and Melilla for the 2003 Algerian tsunami.

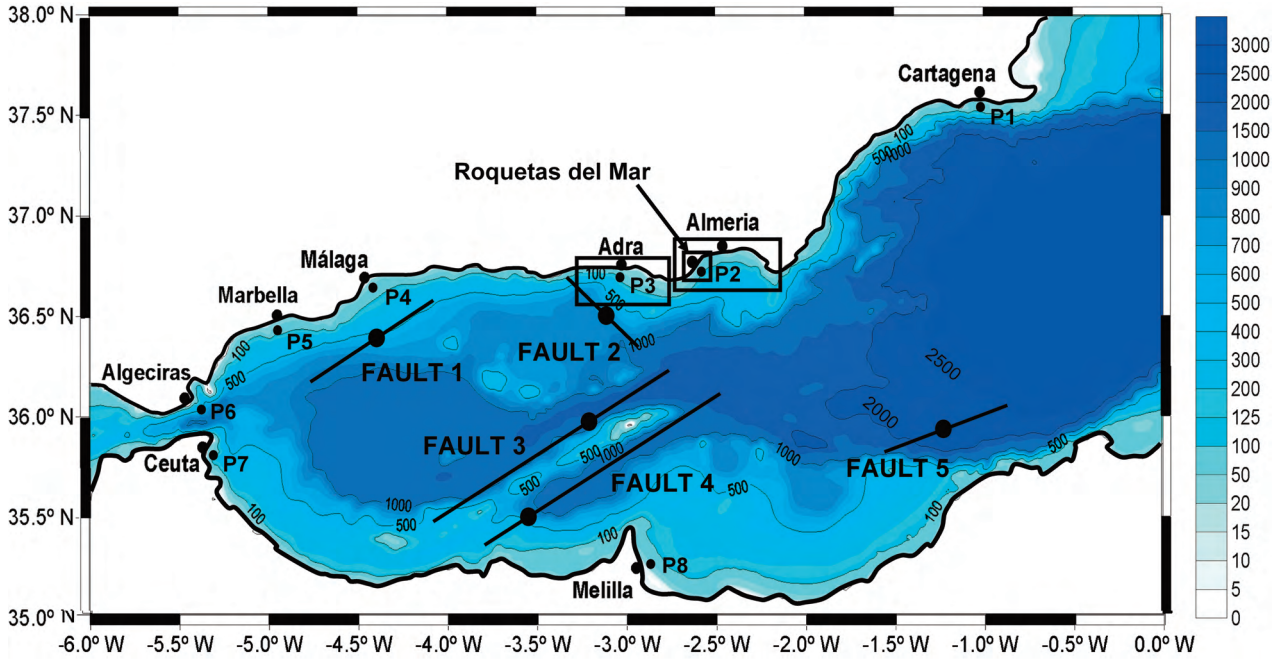

Figure 5. Location map showing the global and detailed grids and the potential tsunamigenic sources.

parameters were proposed by Meghraoui *et al.* (2004). In Figure 5 the five potential tsunamigenic sources selected for the Alborán Sea area are shown.

Tsunami Source Model

In this study, the offset is assumed to be a vertical ascendant movement generated by submarine earthquakes of tectonic origin, which are associated with the five selected potential sources. It is also assumed that the sources are simple straight faults with a focus located at the middle point (see Figure 5). The fault plane mechanism is defined by: (1) the source location; (2) the plane area of the ground displacement, S; (3) the average offset or vertical dislocation, D; and (4) the velocity of the displacement, ξ (t). Figure 6 shows a diagram of the bed movement.

The most widely used quantitative measure of the strength of an earthquake has been its magnitude (M_s). However, it is well-known that there is difficulty in relating magnitude to other important source characteristics such as strain-energy release, fault offset, stress drop and source dimensions, etc

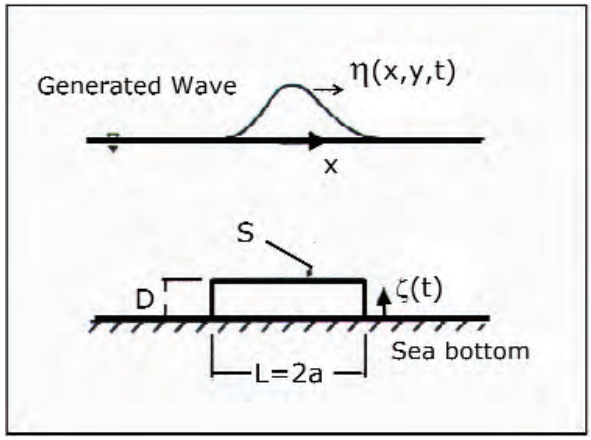

Figure 6. Schematic sea bottom displacement.

(Kanamori & Anderson 1975). For large earthquakes, the seismic moment denoted M_o, is defined as:

$$M_0 = \mu S D \quad (1)$$

in which μ= rigidity of the medium (μ= 3 – 4 A 10^{11} dine – cm^2).

Tsunamigenic earthquakes of tectonic origin are those submarine earthquakes on shallow faults and of large magnitude. As such, tsunamigenic earthquakes are most conveniently measured by seismic moment. In fact, tsunami records in the Pacific have been correlated with and used to calibrate seismic moments (Kanamori 1977).

The number of occurrences of earthquakes with seismic moment, M_0, greater than or equal to m_0 has been shown to be given as:

$$N(m_0) = \alpha m_0^{-\beta} \quad (2)$$

where α and β are numerical constants determined from earthquake records (Kanamori & Anderson 1975; Molnar 1979; Fundación Leonardo Torres Quevedo 1997). Equation (2) will be used to determine the probability distribution function of seismic moment in the section 'probabilistic model for tsunamigenic earthquakes'.

Important physical dimensions of an earthquake are the offset: vertical dislocations and, length and width of ground dislocation. The empirical relation between the seismic moment M_o and the source plane area, S, is given as:

$$M_0 = C_1 S^{3/2} \quad (3)$$

in which C_1= 1.23 A 10^7 dyne – cm^2 width S measured in km^2 (Kanamori & Anderson 1975).

In order to relate seismic moment, M_o, to Richter magnitude, M_s, different authors have proposed empirical relations. Based on earthquake data, the following empirical relationship was obtained for the Azores-Gibraltar-Alborán Sea area (Mezcua *et al.* 1991):

$$\text{Log } M_0 = 1.16\, M_s + 17.93 \quad (4)$$

An expression that can be used to relate M_s to source parameters.

Regarding the dimensions of the plane area of the ground displacement, S (S= L*W), where L is the fault length and W the fault width, a constant scale factor L/W for each fault, based on the maximum scale factor $(L/W)_{max,}$ has been assumed. The maximum width of the fault is approximately the thickness of the seismogenetic crust, due to the steep angle of the dip in Alboran Sea faults (maximum widths between 13 and 20 km). The maximum lengths of the potential faults are between 30 and 130 km. The scale factor (L/W) for these faults has been defined between 3 and 4 in this work. This is in agreement with Papazachos *et al.* (1986) with a scale parameter of $(L/W)_{max}$ ~3 for other areas in the Mediterranean with small magnitudes (M_s<5.5), Scholz (2002) with a scale parameter of (1<L/W<10), and Kajiura & Shuto (1992) with a scale parameter of (4<L/W<8) for large seismic sources with (L> 400km).

In the literature different source mechanism models for seafloor deformations have been proposed, based on linear elastic dislocation theories (e.g., Mansinha & Smylie 1971; Okada 1985) which related different source parameters (strike, dip, slip, rake, focus depth, width). In a similar method to other authors studying tsunami hazard assessment (e.g., Levian & Nosov 2008; Choi *et al.* 2005; Hammack 1972) an impulsive fault plane model has been assumed, where the seafloor deforms instantaneously and the entire fault line also ruptures simultaneously. In this study an elliptical ground displacement in plan view is assumed that provides only positive initial displacements because the magnitude of tsunamis in this zone is reduced (maximum tsunami wave elevation), and the effect of the initial dipole system was not relevant to the results. It simplifies the numerical simulations and the interpolation of data to generate the probabilistic inundation maps. In addition to the methodology proposed in this work, another scope is a comparative analysis in order to determine which areas are more exposed to tsunami hazard along the Alboran Sea. In this frame the elliptical source is an appropriate approximation.

In this study an elliptical ground displacement in plan view is assumed, with an exponential time-displacement function defined as:

$$\zeta(t) = D\,(1-e^{-\alpha t}) \quad 0 < t < t_G \quad (5)$$

with $\alpha = 1.1/t_c$, where t_c is the time to rise 2/3 D (t_c~1 – 20 s.) and t_G is the total generation time, a

parameter assumed to generate an instantaneous bottom displacement (Hammack 1972). D obtained from equation (1), is the plane area of the ground displacement, S is obtained from equations (3) and (4), and the strike angle is defined for the fault orientation (Figure 5).

The study of the finite duration of the earthquake process and the influence of tsunami source areas have been studied by several authors (e.g., Hammack 1972; Levian & Nosov 2008). Hammack (1972), who, using laboratory experiments, analyzed the influence of t_c and t_g for tsunami generation. This author proposed that three nondimensional parameters of bed deformation are important in defining the characteristics of the waves in the generation area: D/h, which represents an amplitude scale of the disturbance, where h is the mean water depth in the source; b/h which represents a size scale of the disturbance, where b is the source width; and the time-size ratio $T_{ad}= t_c \sqrt{gh/b}$ where g is the acceleration of gravity. Hammack (1972) proposed an impulsive bed deformation when $T_{ad} < 1$, $D/h<0.2$ and $b/h>3$. In this case the sea surface deforms instantaneously and mimics the seafloor movement, and the linear theory accurately predicts the wave structure in the generation. In order to define t_c and t_G a sensitivity analysis was carried out using numerical simulations for the different sources. In this analysis t_G was not relevant between 30s to 300s because most deformation occurs in time t_c. Based on historical data such as the 2003 Boumerdes-Zemmouri earthquake, the teleseismic study shows that the rupture displacement only lasted 12 seconds (Delouis *et al.* 2004) – one order of magnitude faster than the speed of tsunami wave at the water depth around the rupture zone. In the sensibility analysis t_c ranged between 10 to 20 seconds with similar results. Thus, for the Alboran faults we assumed $t_c= 15$ s and $t_G= 60$ s. Using these values, Table 1 summarizes the nondimensional parameters proposed by Hammack (1972) for each source and 7 Richter magnitudes, and M_s used later for the numerical simulations. In all cases the generation is an impulsive bed deformation.

In accordance with the tsunami source model, the most important parameters that must be determined are the source location and the seismic moment, M_o.

Hydrodynamic Numerical Model

A coupled numerical model (generation and propagation) was applied to tsunami events.

Generation Numerical Model

Many authors have applied an elliptical water surface shape similar to the ground displacement, for the waves near the source (Houston 1980; Lin & Tong 1986; Camfield 1992). This kind of surface water displacement has also been applied in this study, defined as:

$$\eta(x,y,t) = \zeta(t)\left[1-\left(\frac{x}{a}\right)^2-\left(\frac{y}{b}\right)^2\right]^{\frac{1}{2}} \qquad (6)$$

where $\zeta(t)$ is the equation (5), a= L/2, b=W/2 and the coordinate system origin for the x and y axes is located in the middle of the ellipsoid (or source area)

Propagation Numerical Model H2DTSU

For a distant tsunami, travelling distance can be much greater than the characteristic wave length of the tsunami. In these cases, both the frequency dispersion and Coriolis terms can play an important role (Liu & Chio 1994; Liu *et al.* 1994). However, due to the morphological characteristics of the Alborán Sea (see Figure 5) which is a small basin (approximately 400 km long, 200 km wide and water depth less than 2 km) these two qualifications can be discounted.

As tsunamis propagate into shallow water, wave amplitude increases and wave length decreases due to shoaling. The non linear convective inertia force becomes increasingly important while the importance of frequency dispersion diminishes (Liu & Chio 1994; Liu *et al.* 1994; Wang & Liu 2005).

The tsunami propagations in the Alborán Sea were developed using the H2DTSU model. It solves both non linear and linear shallow water equations. Its nesting capabilities make it possible to simulate tsunami generation and propagation from the source zone to a given coastal area, considering the possible inundation of coastal zones. The model is able to

Table 1. Nondimensional parameters in the source zones for the 5 potential sources in the Alboran Sea.

Nondimensional Parameters	M_s	Fault 1 h=650 m	Fault 2 h=600 m	Fault 3 h=1200 m	Fault 4 h=700 m	Fault 5 h=1500 m
D/h		0.0005	0.0005	0.0003	0.0004	0.0002
b/h	5.18	4.6	5	2.5	4.29	2
$t_c\sqrt{gh}/b$		0.4	0.38	0.54	0.41	0.61
D/h		0.0006	0.0007	0.0003	0.0006	0.0003
b/h	5.5	6.2	6.67	3.33	5.71	2.67
$t_c\sqrt{gh}/b$		0.3	0.29	0.41	0.31	0.45
D/h		0.0009	0.001	0.0005	0.0009	0.0004
b/h	5.88	6.2	6.67	3.33	5.71	2.67
$t_c\sqrt{gh}/b$		0.3	0.29	0.41	0.31	0.45
D/h		0.001	0.0013	0.0007	0.0011	0.0005
b/h	6.23	9.23	10	5	8.57	4
$t_c\sqrt{gh}/b$		0.2	0.19	0.27	0.21	0.3
D/h		0.002	0.0016	0.0008	0.0014	0.0007
b/h	6.58	12.31	13.33	6.67	11.43	5.33
$t_c\sqrt{gh}/b$		0.15	0.14	0.2	0.16	0.23
D/h		0.0023	0.0025	0.0013	0.0021	0.001
b/h	6.93	15.38	16.67	8.33	14.29	6.67
$t_c\sqrt{gh}/b$		0.12	0.12	0.16	0.12	0.18
D/h		0.0028	0.003	0.0015	0.0026	0.0012
b/h	7.28	21.54	23.33	11.67	20	9.33
$t_c\sqrt{gh}/b$		0.09	0.08	0.12	0.09	0.13

capture near shore features of tsunami propagation with higher grid and time resolution and at the same time maintain computational efficiency. This model has been applied in different tsunami cases (e.g., Indonesia 2004, Tumaco, Colombia 1979, Cadiz 1755, see Otero 2003). The model has been validated with the benchmark cases selected in the framework of the EU TRANSFER Project (2006–2009).

The model equations are solved by an implicit finite difference method (Leendertse 1970). As a temporal initial condition, the model used the elliptical deformation of the water surface presented by the relations (5) and (6). An absorbing boundary condition is employed for the seaward boundary and a flooding condition is implemented in the coastline.

Grid Scheme Layout

A global propagation grid measuring 440 × 290 km^2 was adopted (see Figure 5). The numerical computational mesh size and time-step size were fixed, $\Delta x=\Delta y=$ 1000 m, $\Delta t=$ 0.5 s for the wave generation ($t< t_G$) and $\Delta t=$ 5 s for propagation ($t> t_G$). In order to reduce numerical errors, the spatial grid size should be such that one local wavelength includes more than 20 grid points. Therefore, a middle spatial grid size was adopted, $\Delta x=\Delta y=$ 200 m for a water depth less than 50 m. Finally, a finer grid size was adopted, $\Delta x=\Delta y=$ 50 m for Roquetas del Mar (Almería) to generate flooding maps in this location (high resolution bathymetry provided by the Spanish Environmental Ministry). The global

mesh, the two middle grids (Adra and Almería) and the finer grid in Roquetas del Mar are shown in Figure 5.

More than 150 tsunami cases have been modelled using the H2DTSU numerical model for the different sources with different magnitudes. These numerical simulations have been used to interpolate the synthetic cases generated by the probabilistic model based on Monte-Carlo simulations. A propagation tsunami example generated in fault 5 (M_s= 7.5), is shown in Figure 7, where the computed water surface appears at t= 18 min and t= 33 min.

Probabilistic Tsunami Hazard Analysis (PTHA)

The tsunamigenic earthquake is not a deterministic phenomenon; both source location and seismic moment, M_o, have to be defined as random variables. Since the occurrence of future tsunamis is difficult to predict, the tsunami hazard assessment must be based on probabilistic considerations. One of the elements involved is the probability of tsunami inundation of various levels at a given place in a given return period. This probability is generally referred to as hazard.

Eight points (see Figure 5) along the Alborán Sea coast were selected to perform the hazard analysis. The PTHA consists of: (1) a Monte-Carlo simulation, which is based on a probabilistic model in order to obtain the synthesized record of tectonic deformations of the seabed; (2) the tsunami source model, which permits us to relate the physical dimensions (S, D) of the displaced bottom source [equations (1) and (2)]; and (3) the hydrodynamic numerical model which is used to simulate propagation of the tsunami caused by each of the synthetic seabed deformations.

Probabilistic Model for Tsunamigenic Earthquakes

In order to obtain the synthesized record of seabed deformations, it is necessary to define the three basic random variables involved in hazard analysis: (1) the occurrence of tsunamigenic earthquakes; (2) the earthquake source; and (3) the seismic moment, M_o.

The tsunami mean frequency of occurrence was obtained based on the eight events which occurred during the last 200 years, as there is no historical catalogue of tsunamis before 1800. Therefore, it is assumed that one tsunami event occurs every 25 years on average.

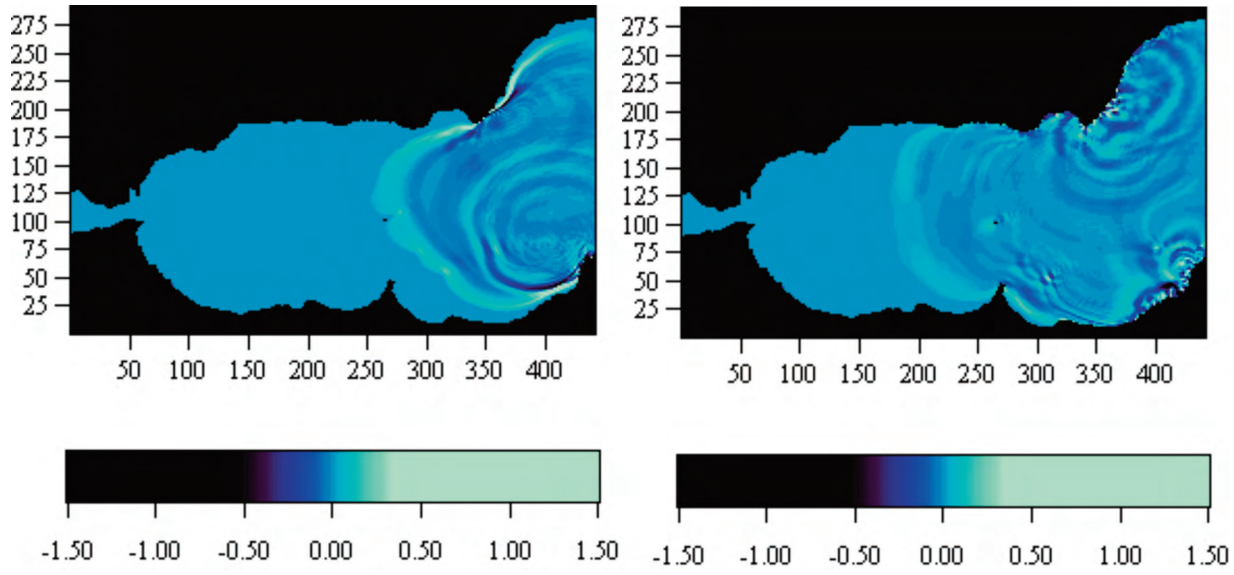

Figure 7. Propagation example tsunami wave elevation (t= 18 and 33 min), epicenter at fault 5, with M_s= 7.5.

As stated previously, five potential individual faults were selected. However, the probability of the occurrence of tsunamigenic earthquake events in each one of these is different. In order to obtain these probabilities, the following hypotheses are assumed: (1) the faults are independent and once every 25 years an event occurs in one of the five faults; (2) a tsunamigenic earthquake originates from a single, well-defined, straight fault; (3) earthquakes can occur anywhere along a fault with equal likelihood but the focal point is located in the middle of a straight fault (see Figure 5); and (4) the probability of the occurrence of tsunamigenic earthquakes on a specific fault increases with the number of events with Richter magnitudes ($M_s \geq 5$) and focal depths ($D_f < 50$ km). Figure 8 shows the probability function obtained for each one of the potential faults.

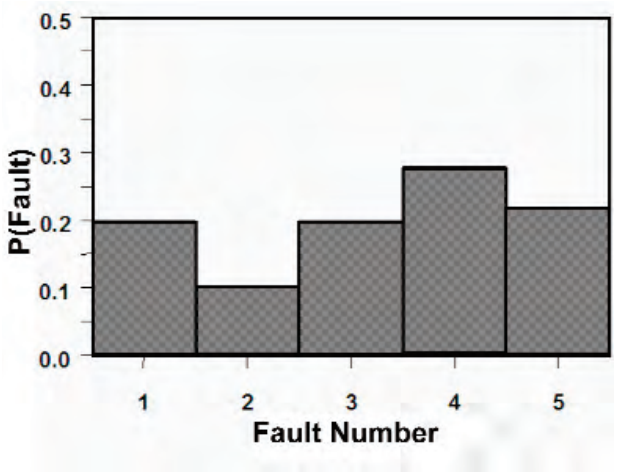

Figure 8. Probability function of tsunami occurrence in potential faults.

The probability distribution function, of $F_{Mo}(m_o)$ was determined, using equation (2) by Lin (1982), as:

$$F_{Mo}(m_o) = \left[1 - \left[\frac{m_{ol}}{m_o}\right]^{\beta}\right] \cdot \left[1 - \left[\frac{m_{ol}}{m_{ou}}\right]^{\beta}\right]^{-1} \qquad (7)$$

$$m_{ol} \leq m_o \leq m_{ou}$$

where m_{ol} and m_{ou} are the lower- and upper-bound magnitudes of seismic moment respectively. Equation (7) was applied for the five potential faults, taking into account the empirical relation between M_s and M_o (equation 4), and the seismological data to obtain m_{ol} and m_{ou} and β (see values in Table 2). Using the Gutenberg-Richter Law (1944) that relates the earthquake magnitude with its frequency, the β parameter has been defined in each fault. This law is given by equation (8).

$$\log N = a - bM_w \qquad (8)$$

where N represents the accumulated frequency of the earthquakes with a magnitude higher or equal to M_w (the momentum magnitude). The a coefficient establishes the seismic activity in the zone, while the parameter b is related to the difference between the frequency of large and small earthquakes. The annual rate of earthquakes with a magnitude higher or equal to M_w (λ_{mw} (N/T)), is given by equation (9).

$$\lambda_{m_w} = \exp(\alpha - \beta M_w) \qquad (9)$$

where $\alpha = a \ln(10)$ and $\beta = b \ln(10)$.

Table 2. The lower- and upper-bound magnitudes of seismic moment and β parameter for each potential fault

Fault	Probable Fault	M_{0l} (din -cm)	M_{sl} Richter	M_{0u} (din - cm)	M_{su} Richter	β
1	0.20	$10^{23.73}$	5	$10^{26.65}$	7.5	0.79
2	0.10	$10^{23.73}$	5	$10^{26.65}$	7.5	0.91
3	0.20	$10^{23.73}$	5	$10^{26.65}$	7.5	0.70
4	0.28	$10^{23.73}$	5	$10^{26.65}$	7.5	0.78
5	0.22	$10^{23.73}$	5	$10^{26.65}$	7.5	0.66

The time interval has been obtained based on the tsunami catalogue data with 8 events in the past 200 years applied to the full region. However, the time interval due to earthquakes can be assumed to be a Poissonian process. The probability of having the next earthquake in a time interval of t or higher is given by equation (10).

$$P(T)= 1 - \exp(-\lambda t) \quad (10)$$

Generating a random number for the probability, the time of the interval between two consecutive earthquakes could be obtained, where λ is the annual rate of earthquakes obtained from the seismological data with equation (9) for each fault. As the calculation of the time interval in this way is based in the seismological register (1916–2006), which is a short period of time, at the end it has to be assumed that the frequency of tsunami events is as based on the historical events of the last 200 years. Both approximations were tested with insignificant differences and the authors decided to use the frequency based on the historical tsunami events.

Note that the procedure of extrapolating data obtained for 200 years on a long period of 500 years or more has to be considered carefully and in some cases may be wrong. This extrapolation is more critical with low accuracy in areas with an important range of seismic magnitudes combining catastrophic and small tsunamis. For these cases longer catalogues from historical events (palaeo-tsunamis, etc) are necessary in order to improve prognostics. However, in where we do not have catastrophic tsunamis with a large range of magnitudes, with no relevant differences in maximum tsunami wave elevation between 1,000 – 5,000 years return periods, the predictions are not far from reality, as will be shown later.

Application of a Monte-Carlo Method with a Multidimensional Interpolation Method

This method consists of the creation of different synthetic tsunamigenic earthquakes series for the considered faults. Based on the probabilistic characteristics of the sources, and by applying the Monte-Carlo method, synthetic earthquake series are obtained for the faults. The time series corresponding to each fault are integrated to generate a global tsunamigenic earthquake catalogue for the study region. The length of the time series in the present study was selected as 5,000 years. In order to derive confidence bands, for the maximal tsunami-wave elevation, the present methodology suggests performing 500 Monte-Carlo time series of 5,000 years each series.

The steps followed in the Monte-Carlo simulation for one time series are as follows:

- Every 25 years a tsunami event has been generated.
- Generation of a random number for the probability, in order to select a generation fault based on the fault probability (Figure 8).
- Generation of a random number for the probability of the seismic moment and computation of M_o for the selected fault using the probability distribution function, $F_{Mo}(m_o)$ (equation (7)).
- Computation of the rupture area (S) and the average offset or vertical dislocation, D; using equation (1) and equation (3) based on the selected M_o.

Once the synthetic earthquake series are derived (200 tsunami events in 5,000 years), they are all joined in a single global synthetic catalogue.

However, the 150 tsunami cases, executed with the H2DTSU numerical model for the different sources and magnitudes have been used to interpolate the maximum tsunami wave elevation in selected points in water depths of 6 m to 10 m along the Alboran coast, and the coastal area in the location of Adra City (Almería). For each tsunamigenic earthquake produced in the synthetic tsunami series, the maximum tsunami wave elevation is obtained applying a multidimensional interpolation method using numerical simulations. In this way, the time series of the aforementioned variable can be derived for the whole coastal region. Therefore, this time series can be used to perform a

statistical analysis of the selected variables and derive maps with an associated return period. To do this, once the time series have been reconstructed in each middle and high resolution grid node, these data are sorted in an ascendant form. An accumulated probability is assigned to each organized scenario. This is given by its position, *i*, see equation (11).

$$P_i = i / (m + 1) \quad (11)$$

where *i* represents the data position and *m* represents the total number of data. The distribution function of the analyzed parameter v_i is given by equation (12).

$$FZ_i(\nu) = 1 - \exp(-\lambda(1-P_i)) \quad (12)$$

where $FZ_i(\nu)$ is the annual excess probability and λ is the tsunamigenic earthquakes annual rate. For the computation of return period T_r the following expression is used:

$$T_r = \frac{1}{FZ(\nu_r)} \quad (13)$$

where T_r represents the mean number of years in which the variable v_r exceeds a given value.

For each return period and each synthetically generated catalogue, a value of the study variable is obtained in all the grid nodes. Therefore, for a given return period, the analysed variable can be mapped in the high resolution grid in Roquetas del Mar.

If several synthetically generated earthquake catalogues are performed, the value of the analyzed parameter for a given return period will present a mean value and a variance. Computing the distribution function of the values obtained for the given return period, the value for a given return period with a given confidence can be obtained.

Results

The PTHA is represented by curves, which permit the maximal tsunami-wave elevation and the maximum limits of inundation impacts in given sites along the Alborán seacoast to be obtained at two confidence levels (50% and 99.99%) and return period (years). As an example of these curves, in Figure 9 the maximum tsunami wave height for different return periods in Adra at 6 m water depth is shown. The inundation contours for 500 and 1,000 year return periods in Roquetas del Mar (Almeria) are also presented in Figure 10. An interesting aspect resulting from local effects of the sea bottom configuration and coastal contours in the wave propagation is seen in the Roquetas del Mar beach, where the tsunami wave energy concentration generated by shoaling is important due to its location in a large coastal salient (see Figure 5). On Roquetas Beach a horizontal penetration of the tsunami waves reaches the boardwalk for the 500-year return period (see Figure 10). In contrast, in the city of Almería (Figure 5) which is located close to Roquetas at the end of the bay, the tsunami energy is redistributed and the maximum wave elevation is reduced (less than 20 cm for the 500-year return period in 6 m water depth).

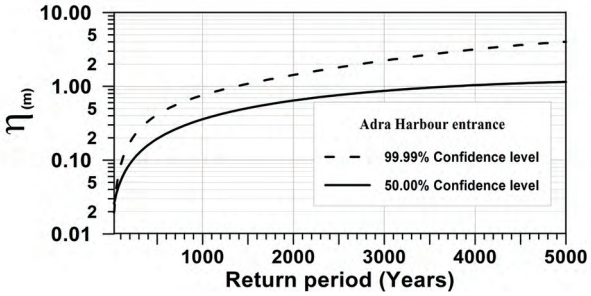

Figure 9. PTHA example. The maximum tsunami wave height in the city of Adra at 6m water depth.

In Figure 11, for a return period of 500 years, the maximum tsunami wave height for different places along the Alborán Sea in water depths of 6 m is shown. This figure shows the most vulnerable areas near Adra, Málaga and Melilla.

Conclusions

- An indirect statistical method has been proposed to estimate tsunami hazard assessment and has been applied along the Alborán seacoast (southeastern Spanish coast). This method can be summarized as: (1) analysis of the global neotectonic setting, with the geodynamic processes and seismicity of

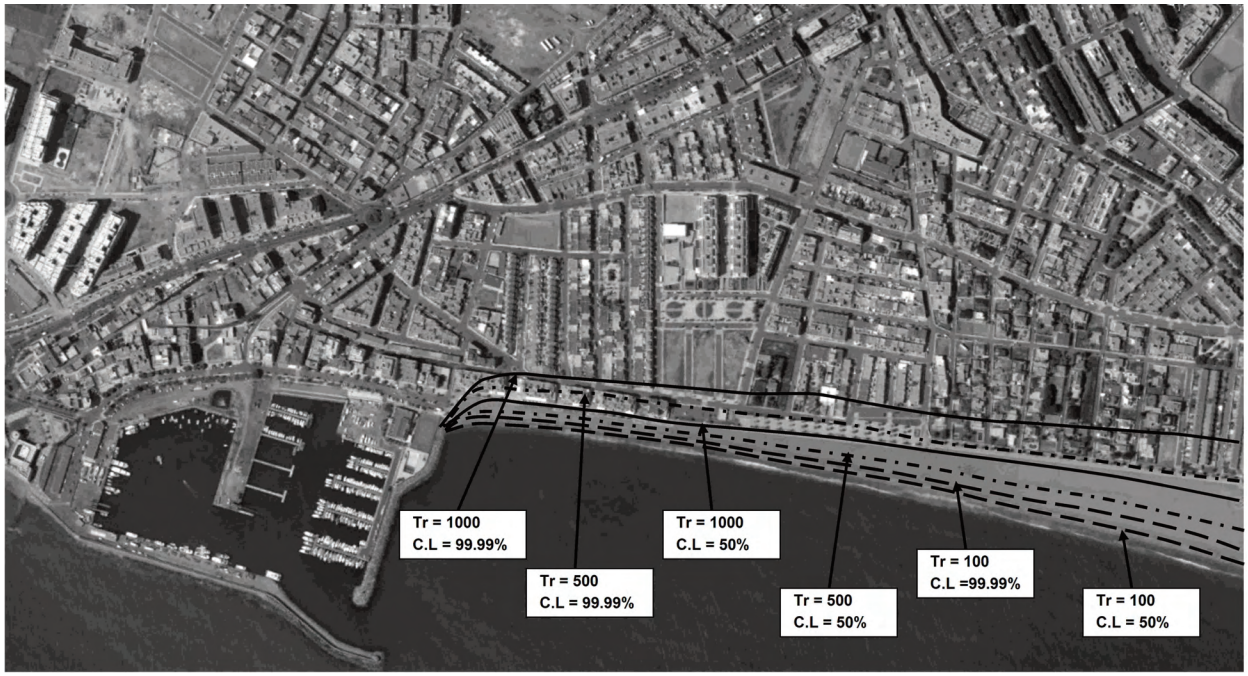

Figure 10. Inundation contours for different return periods in the city of Roquetas del Mar (Almeria) (50% confidence level in solid line, the 99.9% confidence level in broken line). Aerial image of Roquetas del Mar is courtesy of Google Earth.

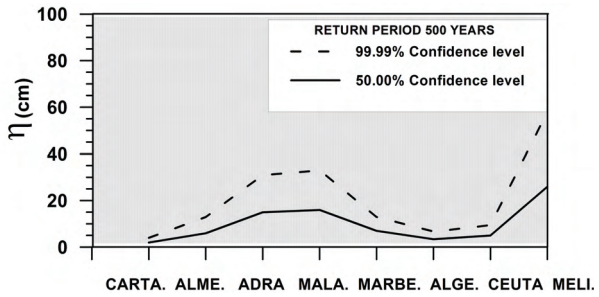

Figure 11. Tsunami hazard assessment. Maximum tsunami wave height in 6m water depth for a return period of 500 years in Cartagena, Almería, Adra, Málaga, Marbella, Algeciras, Ceuta and Melilla.

the region; (2) tsunami source model; (3) generation of a numerical data base of tsunami events using a numerical model; (4) probabilistic model based on Monte-Carlo simulations in order to generate a synthetic tsunami catalogue; and (5) a multidimensional interpolation method applied to combine the numerical data base with the synthetic catalogue to produce inundation maps.

- Given the global neotectonic setting, and the geodynamic processes and the seismicity of the Alborán Sea, the tsunamis generated in the area present a medium-to-low hazard.
- Five potential tsunamigenic faults have been determined in the area (Figure 5).
- Tsunami hazard assessment in different sites along the Alborán Sea has been computed using simple tsunami source, hydrodynamics, and hazard models.
- Due to morphologic characteristics and the setting of potential faults, zones close to Málaga, Adra and Melilla have a larger tsunami wave elevation than the rest of the Alborán Sea locations.
- This is a first approach for a probabilistic tsunami hazard analysis in the area. Further research is necessary to identify more historical events in order to define a better frequency of tsunami occurrence in the Alborán Sea. Also, more studies are required to better characterize the source mechanisms.

Acknowledgements

This research has been partially supported by the 'Comisión Interministerial de Ciencia y Tecnología' under the project MAR96-1135 and the European TRANSFER project (Tsunami Risk ANd Strategies for European Region), sixth framework programme 'Assessment and Reduction of Tsunami Risk in Europe'. The authors are grateful for stimulating reviews by Professor Ahmet Yalçıner and other two anonymous reviewers. English of the final text is edited by John A. Winchester.

References

Alami, S.O. & Tinti, S. 1991. A preliminary evaluation of the tsunami hazards in the Moroccan coasts. *The International Journal of the Tsunami Society* **9**, 31–38.

Alasset, P.J., Hébert, H., Maouche, S., Calbini, V. & Meghraoui, M. 2006. The tsunami induced by the 2003 Zemmouri earthquake (Mw= 6.9, Algeria): modelling and results. *Geophysical Journal International* **166**, 213–226.

Álvarez-Gómez, J.A., Olabarrieta, M., González, M., Otero, L., Carreño, E. & Martínez-Solares, J.M. 2010. The impact of Tsunamis on the Island of Majorca induced by North Algerian Seismic Sources. *The Turkish Journal of Earth Sciences* **19**, 367–383.

Annaka, T., Satake, K., Sakakiyama, T., Akakiyama, T., Yanagisawa, K. & Shuto, N. 2007. Logic-tree approach for probabilistic tsunami hazard analysis and its applications to the Japanese coasts. *Pure and Applied Geophysics* **164**, 577–592.

Camfield, F.E. 1992. Tsunami effects on coastal structures. *Journal of Coastal Research Special Issue, Coastal Hazards* **12**, 177–187.

Choi, B.H., Pelinovsky, E., Lee, H.J. & Woo, S.B. 2005. Estimates of tsunami risk zones on the coasts adjacent to the East (Japan) Sea based on the synthetic catalogue. *Natural Hazards* **36**, 355–381.

Scholz, C.H. 2002. *The Mechanics of Earthquakes and Faulting*. 2nd Edition, Cambridge University Press,Cambridge, UK.

Cramer, C.H., Petersen, M.D. & Reichle, M.S. 1996. A Monte Carlo approach in estimating uncertainty for a seismic hazard assessment of Los Angeles, Ventura, and Orange counties. California. *Seismological Society of America Bulletin* **86**, 1681–1691.

Delouis, B., Vallée, M., Meghraoui, M., Calais, E., Maouche, S., Lammali, K., Mahsas, A., Briole, P., Benhamouda, F. & Yelles, K. 2004. Slip distribution of the 2003 Boumerdes-Zemmouri earthquake, Algeria, from teleseismic, GPS, and coastal uplift data. *Geophysical Research Letters* **31**, L18607 1–4.

Dewey, J.F., Pitman, W.C., Ryan, W.B.F. & Bonnin, J. 1974. Plate tectonics and the evolution of the Alpine system. *Geological Society of America Bulletin* **84**, 3137–3180.

Ebel, J.E. & Kafka, A.L. 1999. A Monte Carlo approach to seismic hazard analysis. *Seismological Society of America Bulletin* **89**, 854–866.

Fundación Leonardo Torres Quevedo 1997. *Estudio de riesgo de inundación y evaluación de daños por acción de maremotos en el litoral del sureste español (Mar de Alborán)*. Ocean & Coastal Research Group, Universidad de Cantabria.

Geist, E. L. & Parsons, T. 2006. Probabilistic analysis of tsunami hazards. *Natural Hazards* **37**, 277–314.

Gutenberg & Richter, C.F. 1944. Frequency of earthquakes in California. *Seismological Society of America Bulletin* **34**, 185–188.

Hammack, J.L. 1972. *Tsunamis. A Model of Their Generation and Propagation*. California Institute of Technology. Report N. KH-R-38, 337–353.

Houston, J.R. 1980. *Type 19 Flood Insurance Study: Tsunami Predictions for Southern California*. Technical report HL-80–18, US Army Engineer, Waterways Experiment Station, Vicksburg, Miss.

Iida, K. 1963. Magnitude, energy and generation and mechanisms of tsunamis and a catalogue of earthquakes associated with tsunamis. *Proceedings of the 10th Pacific Science Congress Symposium. International Union of Geodesy and Geophysics U.G.G.I., Monograph* **24**, 7–18.

Iida, K. 1970. The generation of tsunamis and the focal mechanisms of earthquakes. *In*: Adams, W.M. (ed), *Tsunamis in the Pacific Ocean, Honolulu, Hawaii*. East-West Center Press, 3–18.

Kajiura, K. & Shuto, N. 1992. *Tsunami. Handbook of Coastal and Ocean Engineering, Vol. 3: Wave Phenomena and Coastal Structures*. Golf Publishing Company, 395–418.

Kanamori, H. 1977. The energy release in great earthquakes. *Journal of Geophysical Research* **82(20)**, 2981–2987.

Kanamori, H. & Anderson, D.L. 1975. Theoretical basis of some empirical relations in seismology. *Seismological Society of America Bulletin* **65**, 1073–1095.

Leendertse, J.J. 1970. *A Water-quality Simulation Model for Well-mixed Estuaries and Coastal Seas: Vol 1. Principles of Computation*. RM-6230-RC. Rand Corporation, Santa. Monica, California.

Levian, B. & Nosov, M. 2008. *Physics of Tsunamis*. *Springer*. DOI:10.1007/978-1-4020-8856-8.

Lin, I.-C. 1982. A preliminary investigation of tsunami,Hazard. *Bulletin* **72**, 2323–2337.

LIN, I.-C & TONG, C.C. 1986. Tsunami hazard. *Journal of Engineering Mechanics* **122**, 874–887.

LIU, P.L. & CHO, Y. 1994. *Numerical Simulation of Tsunami Propagation and Inundation with Application to Hilo, Hawaii*. School of Civil and Environmental Engineering, Cornell University, Ithaca.

LIU, P.L.-F., CHO, Y.-S., YOON, S.B. & SEO, S.N. 1994. Numerical simulations of the 1960 Chilean tsunami propagation and inundation at Hilo, Hawaii. *In*: El-Sabh, M.I. (ed), *Recent Developments in Tsunami Research*. Dordrecht, Netherlands: Kluwer Academic Publishers, 99–115.

MALDONADO, A., CAMPILLO, A.C., MAUFFRET, A.., ALONSO, A., WOODSIDE, J. & CAMPOS, J. 1992a. Alborán Sea late Cenozoic tectonic and stratigraphic evolution. *Geo-Marine Letters* **12**, 179–186.

MALDONADO, A. & COMAS, M.C. 1992b. Geology and geophysics of the Alborán Sea: an introduction. *Geo-Marine Letters* **12**, 61–65.

MANSINHA, L. & SMYLIE, D.E. 1971. The displacement fields of inclined faults. *Seismological Society of America Bulletin* **61**, 1433–1440.

MEGHRAOUI, M., MAOUCHE, S., CHEMAA, B., CAKIR, Z., AOUDIA, A., HARBI, A., ALASSET, P.J., AYADI, A., BOUHADAD, Y. & BENHAMOUDA, F. 2004. Coastal uplift and thrust faulting associated with the Mw= 6.8 Zemmouri (Algeria) earthquake of 21 May, 2003. *Geophysical Research Letters* **31**, L19605 1–4.

MEZCUA, J., RUEDA, J. & BUFORN, E. 1991. Seismic deformation in the Azores-Alborán Sea region. *Instituto Geográfico Nacional de España. Monografía* **8**, 205–211.

MEZCUA, J. & RUEDA, J. 1997. Seismological evidence for a delamination process in the lithosphere under the Alboran Sea. *Geophysical Journal International* **129**, F1–F8.

MOLNAR, P. 1979. Earthquake reoccurrence intervals on plate tectonics. *Seismological Society of America Bulletin* **69**, 115–133.

MUSSON, R.M.W. 200 Fundación 0. The use of Monte Carlo simulations for seismic hazard assessment in the *U.K. Annali di Geofisica* **43**, 1–9.

OKADA, Y. 1985. Surface deformation due to shear and tensile faults in a half-space. *Seismological Society of America Bulletin* **75**, 1135–1154.

OTERO, L. 2003. *Simulación Numérica de Tsunamis en el Litoral Pacifico Colombiano: Bahía de Tumaco.* Master Thesis, Universidad de Cantabria, Spain [in Spanish, unpublished].

PAPADOUPOULOS, G.A. 2003. Tsunami hazard in the Eastern Mediterranean: strong earthquakes and tsunamis in the Corinth Gulf, Central Greece. *Natural Hazards* **29**, 437–464.

PAPAZACHOS, B.C., KOUTITAS, CH., HATZIDIMITRIOV, P.M., KARACOSTAS, B.G. & PAPAIGANNOV, CH. A. 1986. Tsunami hazard in Greece and the sourrounding area. *Annales Geophysical, A, B*, **1**, 79–90.

RIKITAKE, T. & AIDA, I. 1988. Tsunami hazard probability in Japan. *Seismological Society of America Bulletin* **78**, 1268–1278.

SAVAGE, J.C. 1992. The uncertainty in earthquake conditional probabilities. *Geophysical Research Letters* **19**, 709–712.

UDÍAS, A., LÓPEZ ARROYO, A. & MEZCUA, J. 1976. Seismotectonic of the Azores-Alborán region. *Tectonophysics* **31**, 259–289.

UDÍAS A. & BURFORN, E. 1992. Sismicidad y sismotectónica de las béticas. *Física de la tierra* **4**, 109–123.

WANG, X. & LIU, P.L.-F. 2005. A Numerical investigation of Boumerdes-Zemmouri (Algeria) Earthquake and Tsunami. *Computer Modelling in Engineering and Sciences* **10**, 171–184.

WARD, S.N. 2001. Landslide tsunami. *Journal of Geophysical Research* **106**, 11201–11215.

WOODSIDE, J.M. & MALDONADO A. 1992. Styles of compressional neotectonics in the eastern Alborán Sea. *Geo-Marine Letters* **12**, 111–116.